

Inter-layer valence bonds and two-component theory for high- T_c superconductivity of $\text{La}_3\text{Ni}_2\text{O}_7$ under pressure

Yi-feng Yang,^{1,2,3,*} Guang-Ming Zhang,^{4,5,†} and Fu-Chun Zhang^{6,‡}

¹*Beijing National Laboratory for Condensed Matter Physics and Institute of Physics, Chinese Academy of Sciences, Beijing 100190, China*

²*School of Physical Sciences, University of Chinese Academy of Sciences, Beijing 100190, China*

³*Songshan Lake Materials Laboratory, Dongguan, Guangdong 523808, China*

⁴*State Key Laboratory of Low-Dimensional Quantum Physics and Department of Physics, Tsinghua University, Beijing 100084, China*

⁵*Frontier Science Center for Quantum Information, Beijing 100084, China*

⁶*Kavli Institute for Theoretical Sciences and CAS Center for Topological Quantum Computation, University of Chinese Academy of Sciences, Beijing 100190, China*

(Dated: November 15, 2023)

The recent discovery of high- T_c superconductivity in bilayer nickelate $\text{La}_3\text{Ni}_2\text{O}_7$ under high pressure has stimulated great interest concerning its pairing mechanism. We argue that the weak coupling model from the almost fully-filled d_{z^2} bonding band cannot give rise to its high T_c , and thus propose a strong coupling model based on local inter-layer spin singlets of Ni- d_{z^2} electrons due to their strong on-site Coulomb repulsion. This leads to a minimal effective model that contains local pairing of d_{z^2} electrons and a considerable hybridization with near quarter-filled itinerant $d_{x^2-y^2}$ electrons on nearest-neighbor sites. Their strong coupling provides a unique two-component scenario to achieve high- T_c superconductivity. Our theory highlights the importance of the bilayer structure of superconducting $\text{La}_3\text{Ni}_2\text{O}_7$ and points out a potential route for the exploration of more high- T_c superconductors.

Introduction.— Exploration of high- T_c superconductivity has lasted for almost four decades since the first discovery of cuprate superconductors [1–3]. One of the main ideas is to start from a Mott insulator, suppress the long-range antiferromagnetic order by doping, and create spin singlet pairs whose phase coherence may eventually lead to the high- T_c superconductivity [4]. However, attempts to replicate this doped-Mott-insulator mechanism in nickelates have not been successful despite of intensive experimental investigations [5–7]. An advance is the discovery of the infinite-layer $(\text{Nd,Pr})_{1-x}\text{Sr}_x\text{NiO}_2$ nickelate superconductors [8–11], which have the desired d^9 configuration with almost half-filled Ni- $d_{x^2-y^2}$ orbitals [12–16]. But superconductivity only appears in thin films with the transition temperature below 40 K even under high pressure [17].

More recently, the bilayer $\text{La}_3\text{Ni}_2\text{O}_7$ bulk superconductor with a much higher T_c of about 80 K has been found under high pressure [18–21]. Density functional theory (DFT) calculations predicted a $d^{7.5}$ configuration with an almost fully-filled d_{z^2} bonding band and two $d_{x^2-y^2}$ bands near quarter-filling [18, 22], which is far from the Mott regime. Although many theoretical works [23–32] have been proposed, the key question concerning its high- T_c pairing mechanism remains open.

It is known that the highest T_c of cuprate superconductors is achieved in the trilayer structure of CuO_2 planes within a unit cell [33–35]. Experiments have shown that the outer and inner CuO_2 planes have different hole concentrations [36, 37]. While the outer planes are heavily hole-doped, the inner one is only slightly doped. A composite scenario had been put forward by Kivelson to

understand how this might lead to the highest T_c [38]. This scenario contains a pairing component with a high pairing scale Δ but small or zero superfluid stiffness, and a metallic component with no pairing but high phase stiffness. The two components are strongly coupled by a tunneling matrix element or hybridization. Under proper conditions, a high $T_c \sim \Delta/2$ can be reached [39] by assuming the superconducting transition as the Kosterlitz-Thouless phase transition [40]. In a recent experimental work, Luo *et al.* argued that the outer and inner planes in trilayer $\text{Bi}_2\text{Sr}_2\text{Ca}_2\text{Cu}_3\text{O}_{10+\delta}$ ($\text{Bi}2223$) cuprate superconductors play the role of the pairing and metallic components, respectively, and the unusual phase diagram in which T_c keeps nearly constant in the overdoped region might thus be well explained [41].

Although the application of Kivelson’s composite scenario to the cuprate superconductors may be debated, it motivated us to propose a more realistic two-component theory for the high- T_c mechanism in superconducting $\text{La}_3\text{Ni}_2\text{O}_7$ under high pressure. We argue in this work that the weak coupling picture starting from the DFT single particle band structures with the almost fully-filled d_{z^2} bonding band may not be able to give the high T_c . Rather, the strong on-site Coulomb repulsion favors almost half-filled and localized d_{z^2} electrons on the Ni ions. This, together with the special bilayer structure of $\text{La}_3\text{Ni}_2\text{O}_7$, creates an inter-layer superexchange interaction of d_{z^2} electrons through the apical O- p_z orbital, and further induces local spin singlets with a large pairing energy. We show that their hybridization with near quarter-filled itinerant $d_{x^2-y^2}$ electrons on nearest-neighbor sites may explain the high- T_c superconductivity in pressurized

La₃Ni₂O₇. A minimal effective model is then constructed for more elaborated investigations. Our scenario differs from the picture of the one-band Hubbard model or t - J model for cuprate superconductors [1–3] and points out an alternative route to realize the high- T_c superconductivity by doping into the spin-singlet array [42].

Electronic band structures.— We start with considering the basic lattice structure of superconducting La₃Ni₂O₇ under high pressure, which contains two layers of Ni-O octahedra with shared apical O. The Ni- d orbitals are split into fully-filled t_{2g} orbitals, which are irrelevant for the low-energy physics, and partially-filled e_g orbitals. DFT calculations [18, 22] predict dominant Ni- d_{z^2} and Ni- $d_{x^2-y^2}$ characters near the Fermi energy. These two orbitals are orthogonal on individual Ni ion, but hybridize strongly between the in-plane nearest-neighbor sites through the Ni-O-Ni bond. Due to the bilayer structure, the Ni- d_{z^2} orbitals coupled through the shared apical O- p_z orbital along z axis are further split into bonding and anti-bonding states [28].

As illustrated in Fig. 1(a), we first construct the non-interacting Hamiltonian of Ni- d_{z^2} and $d_{x^2-y^2}$ orbitals for the bilayer structure after integrating out the O degrees of freedom:

$$H_0 = - \sum_{l(ij)s} t_{ij}^d d_{lis}^\dagger d_{ljs} - t_\perp \sum_{is} (d_{1is}^\dagger d_{2is} + h.c.) - \sum_{l(ij)s} t_{ij}^c c_{lis}^\dagger c_{ljs} - \sum_{l(ij)s} (V_{ij} d_{lis}^\dagger c_{ljs} + h.c.), \quad (1)$$

where d_{lis} (c_{lis}) annihilates a Ni- d_{z^2} ($d_{x^2-y^2}$) electron of spin s at site i on layer l , t_\perp accounts for the inter-layer hopping of d_{z^2} electrons via the shared apical O- p_z orbital, t_{ij}^d (t_{ij}^c) gives the onsite energy and in-plane hopping integral of d_{z^2} ($d_{x^2-y^2}$), and V_{ij} describes their hybridization between nearest-neighbor sites which is positive along x direction and negative along y direction. For simplicity, we have neglected all other inter-layer hopping terms that are supposed to be small. In momentum space, the Hamiltonian may be rewritten as

$$H_0 = \sum_{\mathbf{k}s} \Psi_{\mathbf{k}s}^\dagger \begin{pmatrix} \epsilon_{\mathbf{k}}^c & 0 & -V_{\mathbf{k}}^* & 0 \\ 0 & \epsilon_{\mathbf{k}}^c & 0 & -V_{\mathbf{k}}^* \\ -V_{\mathbf{k}} & 0 & \epsilon_{\mathbf{k}}^d & -t_\perp \\ 0 & -V_{\mathbf{k}} & -t_\perp & \epsilon_{\mathbf{k}}^d \end{pmatrix} \Psi_{\mathbf{k}s}, \quad (2)$$

where $\Psi_{\mathbf{k}s}^\dagger = (c_{1\mathbf{k}s}^\dagger, c_{2\mathbf{k}s}^\dagger, d_{1\mathbf{k}s}^\dagger, d_{2\mathbf{k}s}^\dagger)$, $\epsilon_{\mathbf{k}}^d$ and $\epsilon_{\mathbf{k}}^c$ are the dispersions of d_{z^2} and $d_{x^2-y^2}$ electrons, respectively, and $V_{\mathbf{k}} = V(\cos \mathbf{k}_x - \cos \mathbf{k}_y)$ is their momentum-dependent hybridization. The inter-layer coupling t_\perp is site independent along the planar directions and therefore remains a constant.

The above Hamiltonian can be easily diagonalized and gives an almost fully-occupied d_{z^2} bonding band and two $d_{x^2-y^2}$ bands around the Fermi energy. As predicted by DFT, the d_{z^2} antibonding band is above the Fermi energy. The resulting Fermi surfaces in the two-dimensional

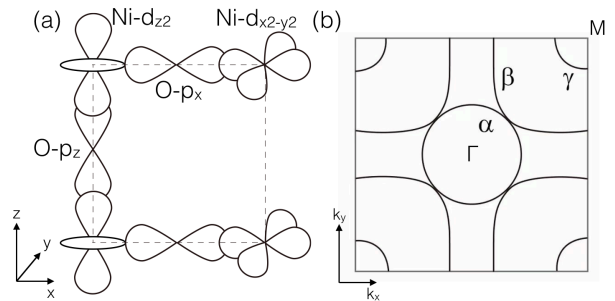


FIG. 1: (a) A schematic diagram of the wave function overlap of bilayer La₃Ni₂O₇ under high pressure, showing the Ni- d_{z^2} and $d_{x^2-y^2}$ orbitals and the O- p orbitals. For clarity, only one of the d_{z^2} and $d_{x^2-y^2}$ orbitals is plotted on each Ni-ion. The y direction is similar to the x direction and not shown. (b) A tentative plot of the DFT Fermi surfaces, showing the γ hole pocket from the d_{z^2} bonding band and the α/β Fermi surfaces from the hybridized $d_{x^2-y^2}$ bands.

Brillouin zone are given in Fig. 1(b), where the d_{z^2} bonding band contributes a small hole pocket γ around M , while the two $d_{x^2-y^2}$ bands hybridize with the d_{z^2} bands and contribute the α and β Fermi surfaces.

Weak coupling picture.— The weak coupling picture starts from the above DFT Fermi surfaces. Hence, the d_{z^2} antibonding band is irrelevant and may be in principle projected out to give an effective three-band model:

$$H_0^{3\text{band}} = \sum_{\mathbf{k}s} \Phi_{\mathbf{k}s}^\dagger \begin{pmatrix} \epsilon_{\mathbf{k}}^c & 0 & -V_{\mathbf{k}}^*/\sqrt{2} \\ 0 & \epsilon_{\mathbf{k}}^c & -V_{\mathbf{k}}^*/\sqrt{2} \\ -V_{\mathbf{k}}/\sqrt{2} & -V_{\mathbf{k}}/\sqrt{2} & \epsilon_{\mathbf{k}}^d - t_\perp \end{pmatrix} \Phi_{\mathbf{k}s}, \quad (3)$$

where $\Phi_{\mathbf{k}s} = (c_{1\mathbf{k}s}, c_{2\mathbf{k}s}, d_{+\mathbf{k}s})^T$, and $d_{\pm\mathbf{k}s} = (d_{1\mathbf{k}s} \pm d_{2\mathbf{k}s})/\sqrt{2}$ describe the bonding (+) and antibonding (-) bands, respectively. To achieve high T_c of about 80 K, the pairing interaction should be sufficiently strong. However, because the γ band is almost fully-filled and the α/β bands are far from the Mott regime, the effective three-band model contains only weak electronic correlations. As may be seen in Fig. 1(b), none of the Fermi surfaces is well nested to support a strong pairing interaction for the high- T_c superconductivity.

Effect of electronic correlations.— To include the correlation effect, we start from the original H_0 in Eq. (1) and construct an interacting Hamiltonian:

$$H = H_0 + U \sum_{li} n_{li\uparrow}^d n_{li\downarrow}^d, \quad (4)$$

where U is the onsite Coulomb repulsion of d_{z^2} electrons, and the Coulomb repulsion for $d_{x^2-y^2}$ orbital has been ignored because of their quarter filling. Then the final Hamiltonian H describes two coupled layers of the periodic Anderson lattice model. For more realistic calculations, we may also include a local Hund's rule coupling between d_{z^2} and $d_{x^2-y^2}$ orbitals: $-J_H \sum_{li} \mathbf{S}_{li} \cdot$

\mathbf{s}_{li} , where the spin operators are defined as $\mathbf{S}_{li} = \frac{1}{2} \sum_{ss'} d_{lis}^\dagger \boldsymbol{\sigma}_{ss'} d_{lis'}$ and $\mathbf{s}_{li} = \frac{1}{2} \sum_{ss'} c_{lis}^\dagger \boldsymbol{\sigma}_{ss'} c_{lis'}$, with $\boldsymbol{\sigma}$ being the Pauli matrices. It has been shown that the Hund's rule coupling tends to compete with the hybridization and promote the quasiparticle flat bands [31].

To see the effect of U , we first consider a toy model of two coupled Ni- d_{z^2} orbitals:

$$H_{\text{toy}} = -t_\perp \sum_s (d_{1s}^\dagger d_{2s} + h.c.) + U \sum_l n_{l\uparrow} n_{l\downarrow}, \quad (5)$$

For half filling, we may rewrite the above Hamiltonian in a matrix form in the subspace of a total electron number $N_d = 2$ and a total spin $S^z = 0$:

$$H_{\text{toy}} = \begin{pmatrix} 0 & 0 & -t_\perp & -t_\perp \\ 0 & 0 & t_\perp & t_\perp \\ -t_\perp & t_\perp & U & 0 \\ -t_\perp & t_\perp & 0 & U \end{pmatrix}. \quad (6)$$

It may then be diagonalized to give the ground state energy $E_0 = (U - \sqrt{U^2 + 16t_\perp^2})/2$ and the wave function:

$$|\text{GS}\rangle = \frac{1}{\sqrt{1 + \alpha^2}} \left(\frac{|20\rangle + |02\rangle}{\sqrt{2}} + \alpha \frac{|\uparrow\downarrow\rangle - |\downarrow\uparrow\rangle}{\sqrt{2}} \right), \quad (7)$$

which is a superposition of the inter-layer spin singlet and two doubly-occupied states. Their relative weight is determined by the parameter $\alpha = \sqrt{x^2 + 1} + x$ with $x = U/4t_\perp$. Thus for $U \ll 4t_\perp$, we have $\alpha \rightarrow 1$ and $|\text{GS}\rangle \approx (|\uparrow\downarrow\rangle + |\downarrow\uparrow\rangle)/2$, which recovers the doubly-occupied d_{z^2} bonding state, while the anti-bonding state is unoccupied with a higher energy. For $U \gg 4t_\perp$, we have instead $\alpha^{-1} \rightarrow 0$ and $|\text{GS}\rangle \approx \frac{|\uparrow\downarrow\rangle - |\downarrow\uparrow\rangle}{\sqrt{2}}$, which is an inter-layer spin singlet. The ground state energy of the spin singlet is $E_0 \approx -4t_\perp^2/U$, which corresponds to the superexchange energy. Taking for example $U = 5$ eV and $t_\perp = 0.6$ eV [23], the weight of the doubly-occupied state is only about 5 percent. Therefore, even for such a large t_\perp from DFT, the on-site Coulomb repulsion can still effectively suppress double occupancy, enforce almost fully localized Ni- d_{z^2} electrons, and produce an inter-layer spin singlet. It is therefore necessary to start from localized d_{z^2} electrons instead of the almost fully-filled d_{z^2} bonding state.

Strong coupling picture.— Our analysis suggests a strong coupling picture with local inter-layer spin singlets of d_{z^2} electrons. They are further hybridized with the near quarter-filled $d_{x^2-y^2}$ bands. The hybridization may cause some electron transfer from d_{z^2} to $d_{x^2-y^2}$ orbitals, which is equivalent to introduce self-doped holes in d_{z^2} orbitals. On the other hand, despite of the strong hybridization, the d_{z^2} spins cannot be fully screened by $d_{x^2-y^2}$ electrons because of their quarter filling. We are therefore left with both strongly renormalized hybridization bands and a large residual inter-layer superexchange coupling that may mediate the electron pairing [31].

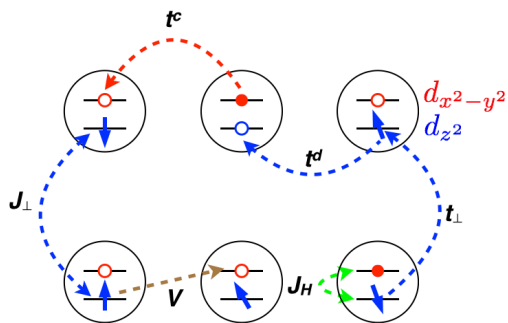


FIG. 2: Illustration of some main low-energy processes. J_\perp (t_\perp) denotes the inter-layer superexchange interaction (hopping) between Ni- d_{z^2} electrons, t^c and t^d are the hopping parameters of $d_{x^2-y^2}$ and d_{z^2} electrons, respectively, their local Hund's rule coupling, and V is their in-plane nearest-neighbor hybridization.

Thus, a minimal effective model may be derived by projecting out only the double occupancy of Ni- d_{z^2} orbital in the interacting Hamiltonian (4):

$$H_{\text{eff}} = J_\perp \sum_i \mathbf{S}_{1i} \cdot \mathbf{S}_{2i} - t_\perp \sum_{is} (d_{1is}^\dagger d_{2is} + h.c.) - \sum_{l(ij)s} t_{ij}^c c_{lis}^\dagger c_{ljs} - V \sum_{lis} (d_{lis}^\dagger \tilde{c}_{lis} + h.c.), \quad (8)$$

where J_\perp is the inter-layer superexchange coupling of d_{z^2} spins and we have defined $\tilde{c}_{lis} = \frac{1}{2}(c_{l,i+\mathbf{x},s} + c_{l,i-\mathbf{x},s} - c_{l,i+\mathbf{y},s} - c_{l,i-\mathbf{y},s})$ to reflect the nearest-neighbor hybridization. Similar to the t - J model for cuprate superconductors, the above model is subject to a local constraint $n_{li}^d = \sum_s d_{lis}^\dagger d_{lis} = 1 - \delta_d \leq 1$, where δ_d counts the self-doped hole density on d_{z^2} orbital. We have dropped the Hund's rule coupling, whose effect is partly included in the renormalization of the hybridization parameter [31]. Other parameters may also be modified by electronic correlations. The small d_{z^2} intra-layer hopping is ignored in the minimal model for simplicity. As in heavily hole-doped cuprates, the intra-layer superexchange interaction is small and dropped because of the near quarter-filled $d_{x^2-y^2}$. Figure 2 gives an illustration of these terms in the low-energy physics. Simply from this effective model, we can already see that $\text{La}_3\text{Ni}_2\text{O}_7$ is a unique system with special characters for exploring exotic many-body quantum phenomena.

Route to high- T_c superconductivity.— Although somewhat different, the similarity compared to the t - J model for hole-doped cuprates suggests a candidate route towards high- T_c superconductivity, with the inter-layer d_{z^2} spin singlets providing a high pairing energy scale given by the inter-layer superexchange interaction J_\perp . To see how this works, we first decouple the superexchange

term in the Hamiltonian (8):

$$J_{\perp} \sum_i \mathbf{S}_{1i} \cdot \mathbf{S}_{2i} \rightarrow -\Delta_d^* \psi_i^d + h.c., \quad (9)$$

where $\psi_i^d = \frac{1}{\sqrt{2}} \sum_{ss'} d_{1is}(i\sigma_{ss'}^y) d_{2is'}$ is the d_{z^2} local inter-layer spin singlet pair and $\Delta_d = \frac{3}{4} J_{\perp} \langle \psi_i^d \rangle$ gives the mean-field self-consistent equation. A second-order perturbation with V yields the (static) $d_{x^2-y^2}$ pairing term:

$$\begin{aligned} H_{\Delta} &= -g_t \frac{\sqrt{2} V^2}{\Delta_d} \sum_i [\tilde{c}_{1is}(i\sigma_{ss'}^y) \tilde{c}_{2is'} + h.c.] \\ &= - \sum_{\mathbf{k}} [\Delta_c^*(\mathbf{k}) \psi_{\mathbf{k}}^c + h.c.], \end{aligned} \quad (10)$$

where $\psi_{\mathbf{k}}^c = \frac{1}{\sqrt{2}} \sum_{ss'} c_{1\mathbf{k}s}(i\sigma_{ss'}^y) c_{2-\mathbf{k}s'}$ for $d_{x^2-y^2}$ electrons, $\Delta_c(\mathbf{k}) = \tilde{\Delta}_c(\cos \mathbf{k}_x - \cos \mathbf{k}_y)^2$ with the proximity induced pairing field $\tilde{\Delta}_c \sim g_t V^2 / \Delta_d$, and $g_t \sim \delta_d$ accounts for Gutzwiller projection to exclude the d_{z^2} double occupancy as in the t - J model. This predicts nodeless s -wave pairing on the d_{z^2} Fermi surface and extended s -wave pairing with possible nodes or gap minima along the zone diagonal on the $d_{x^2-y^2}$ Fermi surfaces. To simplify the discussions, we have ignored the renormalized inter-layer hopping term t_{\perp} , which determines the detailed (anti-)bonding and orbital properties of each Fermi surface but does not affect the primary pairing mechanism. In reality, α and γ Fermi surfaces are from the bonding bands of $d_{x^2-y^2}$ or d_{z^2} orbitals so that their gap functions have the same sign, while the β Fermi surface is from the antibonding band of hybridized $d_{x^2-y^2}$ and d_{z^2} orbitals and its gap function has an opposite sign [43]. Note that despite of the primary role of the d_{z^2} pairing, the induced $d_{x^2-y^2}$ pairing is equally important and the gaps on α and β Fermi surfaces may also be large for sufficiently strong hybridization under high pressure.

The above mean-field equations yield a large $\Delta_d \sim J_{\perp}$ and a transition temperature T_{MF} which is much higher than the true T_c due to the Cooper pair phase fluctuations in two dimension. On the other hand, the d_{z^2} pairs alone have small superfluid stiffness ($\sim \delta_d t^d$) and may not give a large T_c [2]. A different estimate of T_c may be obtained in the composite scenario by following the approach outlined in Ref. [39] to apply a phase twist to the kinetic energy term, $\epsilon_{\mathbf{k}}^c \rightarrow \epsilon_{\mathbf{k}+\mathbf{q}/2}^c$, and calculate the phase stiffness $\rho_s = \partial^2 f / \partial q_x^2$, where f is the free energy density and q_x is the applied phase twist along x direction. Without going into more details, a qualitative analysis yields [39]

$$\rho_s(T) \sim \frac{\tilde{\Delta}_c^2}{T^2} t^c \sim \frac{\delta_d^2 V^4}{J_{\perp}^2 T^2} t^c, \quad (11)$$

which is valid for $g_t V^2 / J_{\perp} \ll T \ll J_{\perp}$. Using the condition, $\rho_s(T_c) = \frac{2}{\pi} T_c$, for the two-dimensional Kosterlitz-

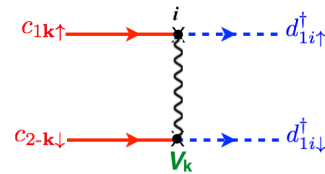


FIG. 3: Illustration of the composite pairing mechanism with strongly coupled d_{z^2} and $d_{x^2-y^2}$ inter-layer spin singlet pairs due to hybridization, where d_{z^2} pairs are more local and have small phase stiffness. $V_{\mathbf{k}}$ denotes their hybridization.

Thouless transition [44], one gets eventually

$$T_c \sim t^c \left(\frac{\delta_d V^2}{J_{\perp} t^c} \right)^{2/3}, \quad (12)$$

which supports a high T_c for finite δ_d as in $\text{La}_3\text{Ni}_2\text{O}_7$ under high pressure and explains the absence of superconductivity at ambient pressure because of the full occupancy of the d_{z^2} bonding band ($\delta_d = 0$). Our theory also predicts that T_c may be enhanced in the low pressure region of the superconductivity by introducing more holes on the d_{z^2} bonding band. On the other hand, applying higher pressure can be regarded as enhancing the hybridization V . While a larger V may promote the phase stiffness, it also tends to compete with the local pairing field, causing non-monotonic variation of T_c [39]. This is confirmed in Monte Carlo simulations of the minimal model [43], in good accordance with experimental observations [18–20].

Our two-component theory represents the lowest-order contribution to the pairing in the presence of self-doped holes in the d_{z^2} orbitals, as illustrated in Fig. 3, with the local inter-layer d_{z^2} spin singlets playing the primary role and attaining phase coherence through hybridization with the metallic $d_{x^2-y^2}$ bands. This mechanism is robust against other perturbations such as inter-layer hybridizations or intra-layer spin interactions. A Hund scenario has been proposed previously in some other superconducting systems [45–52], but we believe it cannot be the primary driving force for the electron pairing in $\text{La}_3\text{Ni}_2\text{O}_7$ since no superconductivity is observed at ambient pressure with fully occupied d_{z^2} bonding band. For the similar reason, we also do not think that spin fluctuations may play an important role. More systematic numerical and experimental studies are needed to settle all the debates.

Discussion and conclusions.— While our theory is motivated by the composite scenario for high- T_c cuprates [38], the two systems have some important differences. First, $\text{La}_3\text{Ni}_2\text{O}_7$ is a multi-orbital bilayer system. This provides a natural basis for the two-component theory, where the more localized d_{z^2} electrons act as the pairing component and the itinerant $d_{x^2-y^2}$ electrons provide the

metallic component. While in cuprate high- T_c superconductors, only one orbital is involved (at least for the Hubbard model), causing some complications in theory. Second, in contrast to the cuprate superconductivity whose parent state is an antiferromagnetic Mott insulator, the high- T_c superconductor $\text{La}_3\text{Ni}_2\text{O}_7$ exhibits no long-range antiferromagnetic order. Rather, it starts with well-formed local spin singlets of Ni- d_{z^2} electrons and superconductivity is induced by doping into the spin-singlet array. This has an obvious advantage, because antiferromagnetic ordering typically competes with the superconductivity, causing failures in previous attempts to find more high- T_c superconductors guided by the cuprate-Mott mechanism.

To summarize, we have proposed a strong coupling picture for $\text{La}_3\text{Ni}_2\text{O}_7$ under high pressure and a two-component pairing mechanism for its high- T_c superconductivity. We show that the weak coupling picture based on almost fully-filled Ni- d_{z^2} bonding band may be incorrect due to the strong on-site Coulomb interaction, and construct a minimal effective model for describing its low-energy physics. This leads to the idea of local inter-layer spin singlet pairing of Ni- d_{z^2} electrons due to a large inter-layer superexchange interaction via the apical O- p_z orbital. High- T_c superconductivity may then be established by hybridization with the metallic $d_{x^2-y^2}$ electrons to induce the global phase coherence. Our theory highlights the importance of the bilayer structure of superconducting $\text{La}_3\text{Ni}_2\text{O}_7$ and provides an alternative route to explore more high- T_c superconductors [42]. Our model provides a basis for more elaborate theoretical investigations.

One of the authors (GMZ) acknowledges stimulating discussions with X. J. Zhou on trilayer cuprates. This work was supported by the Strategic Priority Research Program of the Chinese Academy of Sciences (Grant No. XDB33010100), China's Ministry of Science and Technology (Grant No. 2022YFA1403900), and the National Natural Science Foundation of China (Grant No. 11920101005).

Note added. When preparing this manuscript, we notice several preprints [53–56] which studied a bilayer t - J model with strong inter-layer coupling and considered the possible superconducting pairing symmetry. Several later preprints [57–60] also emphasized the importance of $d_{x^2-y^2}$ pairing for the superconductivity. F.C.Z. was partially supported by the Chinese Academy of Sciences under contract No. JZHKYPT-2021-08.

* yifeng@iphy.ac.cn

† gmzhang@tsinghua.edu.cn

‡ fuchun@ucas.ac.cn

[1] P. W. Anderson, Science 235, 1196 (1987).

- [2] P. A. Lee, N. Nagaosa, and X. G. Wen, Rev. Mod. Phys. **78**, 17 (2006).
- [3] B. Keimer, S. A. Kivelson, M. R. Norman, S. Uchida, and J. Zaanen, Nature **518**, 179 (2015).
- [4] P. W. Anderson, P. A. Lee, M. Randeria, T. M. Rice, N. Trivedi, and F. C. Zhang, J. Phys.: Condens. Matter **16**, R755 (2004).
- [5] M. A. Hayward, M. A. Green, M. J. Rosseinsky, and J. Sloan, J. Am. Chem. Soc. **121**, 8843 (1999).
- [6] A. V. Boris, Y. Matiks, E. Benckiser, A. Frano, P. Popovich, V. Hinkov, P. Wochner, M. Castro-Colin, E. Detemple, V. K. Malik, C. Bernhard, T. Prokscha, A. Suter, Z. Salman, E. Morenzoni, G. Cristiani, H.-U. Habermeier, and B. Keimer, Science **332**, 937 (2011).
- [7] A. S. Disa, D. P. Kumah, A. Malashevich, H. Chen, D. A. Arena, E. D. Specht, S. Ismail-Beigi, F. J. Walker, and C. H. Ahn, Phys. Rev. Lett. **114**, 026801 (2015).
- [8] D. Li, K. Lee, B. Y. Wang, M. Osada, S. Crossley, H. R. Lee, Y. Cui, Y. Hikita, and H. Y. Hwang, Superconductivity in an Infinite-Layer Nickelate, Nature **572**, 624-627 (2019).
- [9] D. Li, B. Y. Wang, K. Lee, S. P. Harvey, M. Osada, B. H. Goodge, L. F. Kourkoutis, and H. Y. Hwang, Phys. Rev. Lett. **125**, 027001 (2020).
- [10] S. Zeng, C. S. Tang, X. Yin, C. Li, M. Li, Z. Huang, J. Hu, W. Liu, G. J. Omar, H. Jani, Z. S. Lim, K. Han, D. Wan, P. Yang, S. J. Pennycook, A. T. S. Wee, and A. Ariando, Phys. Rev. Lett. **125**, 147003 (2020).
- [11] M. Osada, B. Y. Wang, K. Lee, D. Li, and H. Y. Hwang, Phys. Rev. Materials **4**, 121801 (2020).
- [12] V. I. Anisimov, D. Bukhvalov, and T. M. Rice, Phys. Rev. B **59**, 7901 (1999).
- [13] K.-W. Lee and W. E. Pickett, Phys. Rev. B **70**, 165109 (2004).
- [14] M. Jiang, M. Berciu, and G. A. Sawatzky, Phys. Rev. Lett. **124**, 207004 (2020).
- [15] G.-M. Zhang, Y.-F. Yang, and F.-C. Zhang, Phys. Rev. B **101**, 020501(R) (2020).
- [16] Y.-F. Yang and G.-M. Zhang, Front. Phys. **9**, 801236 (2022).
- [17] N. N. Wang, M. W. Yang, Z. Yang, K. Y. Chen, H. Zhang, Q. H. Zhang, Z. H. Zhu, Y. Uwatoko, L. Gu, X. L. Dong, et al., Nat. Commun. **13**, 4367 (2022).
- [18] H. Sun, M. Huo, X. Hu, J. Li, Y. Han, L. Tang, Z. Mao, P. Yang, B. Wang, J. Cheng, D.-X. Yao, G.-M. Zhang, and M. Wang, Nature **621**, 493 (2023).
- [19] Z. Liu, M. Huo, J. Li, Q. Li, Y. Liu, Y. Dai, X. Zhou, J. Hao, Y. Lu, M. Wang, and H.-H. Wen, arXiv:2307.02950.
- [20] J. Hou, P. T. Yang, Z. Y. Liu, J. Y. Li, P. F. Shan, L. Ma, G. Wang, N. N. Wang, H. Z. Guo, J. P. Sun, Y. Uwatoko, M. Wang, G. M. Zhang, B. S. Wang, and J. G. Cheng, arXiv:2307.09865.
- [21] Y. Zhang, D. Su, Y. Huang, H. Sun, M. Huo, Z. Shan, K. Ye, Z. Yang, R. Li, M. Smidman, M. Wang, L. Jiao, and H. Yuan, arXiv:2307.14819
- [22] V. Pardo and W. E. Pickett, Phys. Rev. B **83**, 245128 (2011).
- [23] Z. Luo, X. Hu, M. Wang, W. Wú, and D.-X. Yao, Phys. Rev. Lett. **131**, 126001 (2023).
- [24] Y. Zhang, L.-F. Lin, A. Moreo, and E. Dagotto, arXiv:2306.03231.
- [25] Q.-G. Yang, H.-Y. Liu, D. Wang, and Q.-H. Wang, Phys. Rev. B **108**, L140505 (2023).
- [26] H. Sakakibara, N. Kitamine, M. Ochi, and K. Kuroki,

- arXiv:2306.06039.
- [27] Y. Gu, C. Le, Z. Yang, X. Wu, and J. Hu, arXiv:2306.07275.
- [28] Y. Shen, M. Qin, and G.-M. Zhang, arXiv:2306.07837.
- [29] V. Christiansson, F. Petocchi, and P. Werner, arXiv:2306.07931.
- [30] W. Wu, Z. Luo, D.-X. Yao, and M. Wang, arXiv:2307.05662.
- [31] Y. Cao and Y.-F. Yang, arXiv:2307.06806.
- [32] Y.-B. Liu, J.-W. Mei, F. Ye, W.-Q. Chen, and F. Yang, arXiv:2307.10144.
- [33] B. A. Scott, E. Y. Suard, C. C. Tsuei, D. B. Mitzi, T. R. McGuire, B.-H. Chen and D. Walker, *Physica C* **230**, 239 (1994).
- [34] S. Chakravarty, H.-Y. Kee and K. Volker, *Nature* **428**, 53 (2004).
- [35] A. Iyo, Y. Tanaka, H. Kito, Y. Kodama, P. M. Shirage, D. D. Shivagan, H. Matsuhata, K. Tokiwa, and T. Watanabe, *J. Phys. Soc. Jpn.* **76**, 094711 (2007).
- [36] S. Ideta, K. Takashima, M. Hashimoto, T. Yoshida, A. Fujimori, H. Anzai, T. Fujita, Y. Nakashima, A. Ino, M. Arita, H. Namatame, M. Taniguchi, K. Ono, M. Kubota, D. H. Lu, Z.-X. Shen, K. M. Kojima, and S. Uchida, *Phys. Rev. Lett.* **104**, 227001 (2010).
- [37] S. Ideta, S. Johnston, T. Yoshida, K. Tanaka, M. Mori, H. Anzai, A. Ino, M. Arita, H. Namatame, M. Taniguchi, S. Ishida, K. Takashima, K. M. Kojima, T. P. Devereaux, S. Uchida and A. Fujimori, *Phys. Rev. Lett.* **127**, 217004 (2021).
- [38] S. A. Kivelson, *Physica B* **11**, 61 (2002).
- [39] E. Berg, D. Orgad, and S. A. Kivelson, *Phys. Rev. B* **78**, 094509 (2008).
- [40] V. J. Emery and S. A. Kivelson, *Nature (London)* **374**, 434 (1995).
- [41] X. Y. Luo, H. Chen, Y. Li, Q. Gao, C. Yin, H. Yan, T. Miao, H. Luo, Y. Shu, Y. Chen, C. Lin, S. Zhang, Z. Wang, F. Zhang, F. Yang, Q. Peng, G. Liu, L. Zhao, Z. Xu, T. Xiang, and X. J. Zhou, arXiv:2210.06348.
- [42] Alternative routes to realize high- T_c superconductivity were first considered in M. Gao, Z.-Y. Lu, and T. Xiang, *Physics* **44**, 421 (2015), <https://wuli.iphy.ac.cn/article/doi/10.7693/wl20150701>.
- [43] Q. Qin and Y.-F. Yang, *Phys. Rev. B* **108**, L140504 (2023).
- [44] D. R. Nelson and J. M. Kosterlitz, *Phys. Rev. Lett.* **39**, 1201 (1977).
- [45] A. Georges, L. de' Medici, and J. Mravlje, *Annu. Rev. Condens. Matter Phys.* **4**, 137 (2013).
- [46] J. E. Han, *Phys. Rev. B* **70**, 054513 (2004).
- [47] X. Dai, Z. Fang, Y. Zhou, and F.-C. Zhang, *Phys. Rev. Lett.* **101**, 057008 (2008).
- [48] C. M. Puetter and H.-Y. Kee *Eur. Phys. Lett.* **98**, 27010 (2012).
- [49] G. Csire, B. Újfalussy, and J. F. Annett, *Eur. Phys. J. B* **91**, 217 (2018).
- [50] A. Kostin, P. O. Sprau, A. Kreisel, Y. X. Chong, A. E. Böhrer, P. C. Canfield, P. J. Hirschfeld, B. M. Andersen, and J. C. Séamus Davis, *Nat. Mater.* **17**, 869 (2018).
- [51] S. K. Ghosh, G. Csire, P. Whittlesea, J. F. Annett, M. Gradhand, B. Újfalussy, and J. Quintanilla, *Phys. Rev. B* **101**, 100506(R) (2020).
- [52] M. Roig, A. T. Rømer, A. Kreisel, P. J. Hirschfeld, and B. M. Andersen, *Phys. Rev. B* **106**, L100501 (2022).
- [53] C. Lu, Z. Pan, F. Yang, and C. Wu, arXiv:2307.14965.
- [54] H. Oh and Y. H. Zhang, arXiv:2307.15706.
- [55] Z. Liao, L. Chen, G. Duan, Y. Wang, C. Liu, R. Yu, and Q. Si, arXiv:2307.16697.
- [56] X.-Z. Qu, D.-W. Qu, J. Chen, C. Wu, F. Yang, W. Li, and G. Su, arXiv:2307.16873.
- [57] K. Jiang, Z. Wang, and F. Zhang, arXiv:2308.06771.
- [58] Y.-H. Tian, Y. Chen, J.-M. Wang, R.-Q. He, and Z.-Y. Lu, arXiv:2308.09698.
- [59] D.-C. Lu, M. Li, Z.-Y. Zeng, W. Hou, J. Wang, F. Yang, and Y.-Z. You, arXiv:2308.11195.
- [60] J.-X. Zhang, H.-K. Zhang, Y.-Z. You, and Z.-Y. Weng, arXiv:2309.05726.